Energetics of CO Oxidation on Lanthanide-free Perovskite Systems: the case of Co-doped $SrTiO_3$.

Silvia Carlotto,[a] Marta M. Natile,[b] Antonella Glisenti,[a] Jean-François Paul,[c] Dimitri Blanc,[c] Andrea Vittadini*[b]

The energetics of the catalytic oxidation of CO on a complex metal oxide is investigated for the first time by density functional theory calculations. The catalyst, Co-doped $SrTiO_3$, is modelled using periodically repeated slabs based on the $SrTiO_3$(100) surface. The comparison of the energy profiles obtained for the pure host and for the Co-doped material reveals the actual pathway followed by the reaction, and shows that Co doping enhances the catalytic properties of $SrTiO_3$ by reducing the energy cost for the formation of oxygen vacancies.

1. Introduction

Carbon monoxide is a very toxic gas for human and animals due to its affinity with hemoglobin, and is produced by transportation, industrial, and domestic activities as a result of incomplete combustion.[1] For this reason, the development of gas sensors for CO detection and catalysts for CO oxidation is critical to controlling environmental pollution.[2] Whereas first generation of catalysts, developed to treat automotive exhaust gas, were based on noble metals (Pt, Pd, Rh, Au), the increasing demand of catalytic converters, and the consequent raising of the noble metal price, multiplied the scientific effort to develop new and less costly catalysts requiring a lower usage of critical raw materials (CRMs).[3] This has spurred increasing theoretical and experimental research efforts on the catalytic oxidation of carbon monoxide over new catalysts based on metal oxides.[1,4-10]

Among heterogeneous catalysts, perovskites are particularly interesting because they are active both in CO oxidation and in NO reduction, which makes them suitable for applications in three-way catalysts. Perovskites (general structure ABO_3, where A and B are metal cations, with A having a larger radius than B) represent a versatile class of metal oxides, and are widely used in chemical industry.[11] Several experimental studies showed that perovskites are able to absorb CO and to catalyse its oxidation.[12-14] A unique feature of these materials is the possibility to prepare a wide number of different materials by changing the A and/or B cations over the entire d and f blocks, which makes it possible to tune e.g. the redox and surface properties for specific applications. This allowed to obtain several compounds suitable as active materials in catalytic converters. Unfortunately, most of these contain lanthanide and/or precious metals. An ideal replacement would be a cheap and CRM-free perovskite such as $SrTiO_3$, which is however unable to oxidize CO appreciably.[2] In this regard, it has been recently found that Co-doped $SrTiO_3$ is instead active both in CO oxidation and in NO reduction,[15] which makes it potentially suitable for use in three way catalysts.

Clearly, understanding how doping is able to activate $SrTiO_3$ would give valuable information for the development of new CRM-free catalysts. Studies on the reactivity of $SrTiO_3$ in the presence of surface impurities (such as oxygen vacancies or metal dopants) are however rare and limited to adsorption/desorption ones.[16-21] In a recent paper,[22] some of us investigated the adsorption of small molecules (CO, NO and O_2) on a doped $SrTiO_3$ surface, and found evidence that doping substantially lowers the formation energy of oxygen vacancies. This result stimulated us to investigate the whole catalytic CO oxidation cycle, in order to check whether the low vacancy formation energy could explain the enhanced catalytic properties shown by this system. In this work, we propose and analyse by first principles calculations several CO oxidation mechanisms derived from schemes previously developed for simple metal oxides. In fact, the enhancement of the catalytic properties of simple metal oxides by transition metal doping has been thoroughly investigated by means of first principles calculations in the recent past. This allows to understand in details the microscopic mechanisms of several catalytic reactions. This work represents a first effort of obtaining a comparable degree of comprehension for complex metal oxides such as doped perovskites.

[a] Department of Chemical Sciences, Università di Padova, Via F. Marzolo 1 - 35131 Padova, Italy
[b] Istituto di Chimica della Materia Condensata e di Tecnologie per l'Energia - ICMATE, Via F. Marzolo 1, 35131 Padova, Italy
E-mail: andrea.vittadini@unipd.it
[c] Univ. Lille, CNRS, ENSCL, Centrale Lille, Univ. Artois, UMR 8181 - UCCS - Unité de Catalyse et de Chimie du Solide, F-59000 Lille, France

2. Computational Details

We use the density functional theory (DFT), solving the spin-polarized Kohn-Sham equations with the generalized gradient approximation (GGA), and adopting the PBE exchange-correlation functional.[23,24] The $SrTiO_3$ (100) surface is modelled with a 2 × 2 slab consisting of seven atomic layers of TiO_2 and SrO stacked alternatively and separated by a 19 Å thick vacuum space. This was checked and found to be adequate in previous investigations.[17,18] Only the top (TiO_2-terminated) surface of the slab is used to model adsorption and reactions. The top three atomic layers are relaxed, whereas the bottom four atomic layers are kept fixed to simulate bulk. Effects of both cobalt impurities and oxygen vacancies are also investigated by modifying the composition of the top surface. The theoretical $SrTiO_3$ lattice constant as determined in our previous work (3.93 Å) is used.[25]

Local minima are determined using the PWSCF code of the Quantum-ESPRESSO (QE) software package[26] using the same computational setup of Ref. 22. Transition states (TSs) are located using the VASP code (5.4.1 version)[27,28] and the climbing image nudged elastic band (NEB) method[29] using a cutoff energy E_{cut} = 500 eV and 5 × 5 k-point grid sampling. Under this setup, energy differences computed with the PWSCF and the VASP codes are practically identical. We perform frequency calculations to characterize the TSs and confirm the reaction coordinate.

3. Results and discussion

Predicting the catalytic performance from first principles requires the knowledge of the detailed reaction pathway. In the case of complex materials such as perovskites and other metal oxide systems, this is not an easy task, as many reaction channels are in principle possible. The mechanism of CO oxidation has been the subject of both experimental and theoretical investigations in the cases of lanthanide-containing perovskites[30,31] and of simple metal oxides such as TiO_2, CeO_2, Co_3O_4.[4,7,9,10,32]

In general, in heterogeneous catalysis we can envisage two kinds of mechanisms, i.e., *suprafacial*, in which the surface provides adsorption sites where the reactant molecules are activated; and *interfacial* in which the surface plays an active role in the reaction as a reagent.[1,33] Most of the proposed schemes are of the latter kind, and are based on the Mars–van Krevelen (MvK) mechanism, where CO is first oxidized by the oxygen atoms of the metal oxide surface.[1,34] The subsequent desorption of formed CO_2 molecules leaves behind oxygen vacancies, which are subsequently annihilated by gas-phase O_2 introduced with the feed. This leaves extra O atoms at the surface, which can in turn oxidize further CO molecules, finally closing the catalytic cycle.

In most reactions occurring through the MvK mechanism, the oxidation of the reductant is the rate-determining step, though the details of the mechanism may depend on the specific system.[33] In the present case, after exploring several possibilities, and considering the results of our previous work on the adsorption at the doped $SrTiO_3$ (100) surfaces,[22] we are left with three pathways, which differ in the way the second CO_2 molecule is formed.

We start by examining a pathway (hereafter pathway A), which was proposed originally for CO oxidation on CeO_2 and other metal oxides such as TiO_2 and Co_3O_4.[4,7,9,10] A scheme of this pathway is sketched in Figure 1, where the energy profiles for pure and doped systems are compared. In the Figure 1, the energy is referred to the sum of the total energy of the relaxed clean surface and those of the reactant molecules in the gas phase, which corresponds to the starting A1 point. We now describe in details all the steps on the basis of our outcomes.

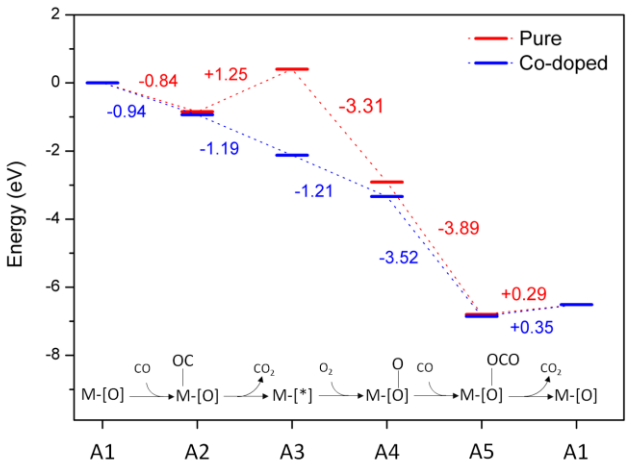

Fig. 1 Reaction energy profiles for CO oxidation on pure (M=Ti) and doped (M=Co) surfaces (pathway A). Energies changes (in eV) are displayed for each step. The structures associated to all the levels are sketched in the scheme at the bottom.

As above pointed out, the first two steps (A1→A2 and A2→A3) involve the adsorption of CO on the metal cation (Lewis acid) site and the oxygen abstraction from the stoichiometric surface by CO, which yields a CO_2 molecule and an oxygen vacancy at the surface. The latter is subsequently (A3→A4) healed by an oxygen molecule, whose protruding end in turn oxidizes a further CO molecule (A4→A5), finally regenerating the perfect surface (A5→A1). The energy profiles resulting from our calculations (see Figure 1) are qualitatively similar to those computed for CO oxidation on other metal oxide surfaces.[4] Apparently, the most relevant difference between the pure and doped systems is the second step, i.e. oxygen abstraction by CO. In fact, Co doping turns it from strongly *endo*thermic (+1.25 eV) to strongly *exo*thermic (-1.19 eV). This provides an explanation for the absence of activity of the pure compound.[2] The cobalt dopant enhances the catalytic properties of $SrTiO_3$ by reducing the energy cost for the formation of oxygen vacancies. Thus, our results confirm previous work[4] pointing out that the efficiency of

MvK-type mechanisms critically depends on the formation energy of the oxygen vacancies. For instance, doping ceria with elements such as Zr or Au promotes catalytic activity for oxidation reactions by decreasing the vacancy formation energy.[35-37] The energetics of all the steps following O abstraction is similar for the doped and the pure systems, except for the adsorption of the oxygen molecule at the vacancy (A3→A4), which is however strongly exothermic in both cases (-3.31 eV vs. -1.21 eV, respectively). Besides, some structural differences are present in the reaction intermediates. For instance, we note that in the pure system the O-vacancy adsorbed O_2 stands perpendicular to the surface plane, with the lower oxygen atom ~0.48 Å below the surface plane, see Figure 2a. In contrast to that, in the case of the doped surface, O_2 is bent towards a Ti cation (see Figure 2b).

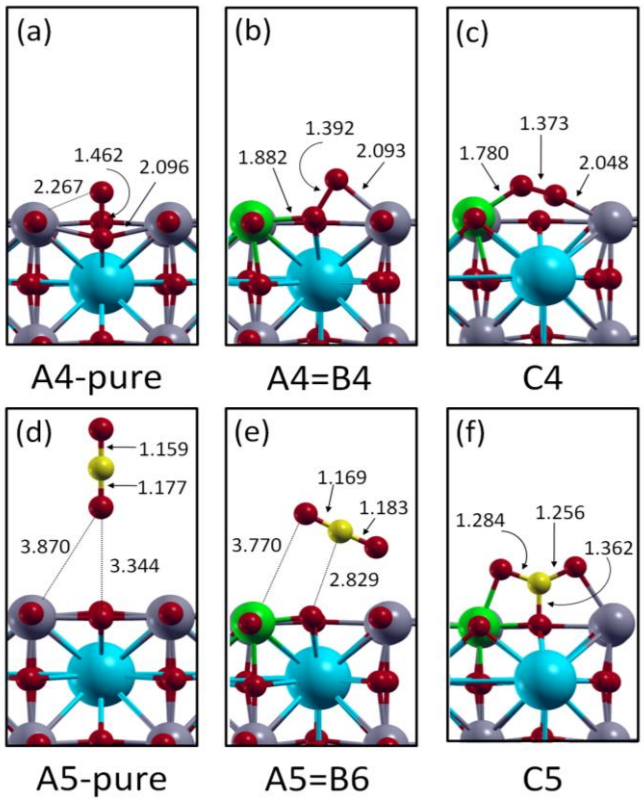

Fig. 2 Relevant intermediates for pathways A, B, and C. Grey spheres are Ti, red spheres are O, cyan spheres are Sr, yellow spheres are C and green spheres are Co. All distances are in Å.

We remark that for both the pure and the doped surfaces the adsorbed O_2 molecule is strongly stretched (by 0.224 and 0.154 Å, respectively), which is indicative of a partial reduction to O_2^{2-}, and makes it available for a chemical reaction with a gas-phase molecule without changing the spin of the system. In fact, placing a further CO molecule over O_2(ads) gives rise to a strongly exothermic (ΔE = -3.5 eV) rearrangement, generating an adsorbed CO_2 molecule (A4→A5). Further, desorption of CO_2 regenerates the perfect surface, finally closing the catalytic cycle. In the pure system, CO_2 is adsorbed perpendicular to the surface and is structurally unperturbed, except for a ~0.01 Å elongation of the C-O bond pointing towards the surface (see Figure 2d). For the doped system, CO_2 lays closer and almost parallel to the surface (see Figure 2e), but its deformation is still small, even though the bond stretching is slightly enhanced and accompanied by a 3° bending. In fact, the CO_2-surface interaction is weak in both cases, which results in the small CO_2 desorption energy, involved in the A5→A1 last step.

We turn now to examine the second pathway (B), which is adapted from a scheme previously proposed for ceria-supported Au nanoparticles.[4] This differs from mechanism A because the second CO_2 molecule is formed through a Langmuir-Hinshelwood-type mechanism, where the O-O bond is attacked by a co-adsorbed CO molecule. In this regard, it was suggested that reducing the strength of the CO-surface interaction could be effective in enhancing the reaction rate. The energy profile for the pure system is not reported (Figure 3, top) because we did not find a stable B5 intermediate.

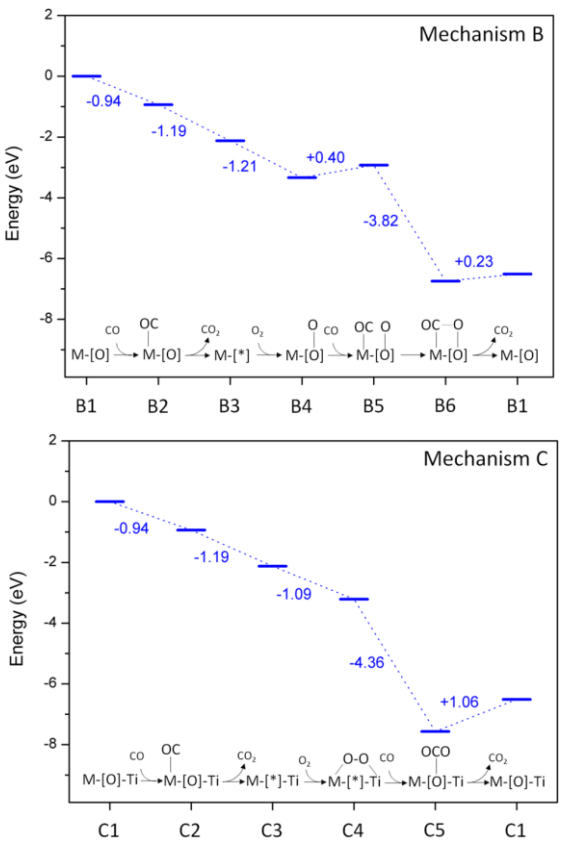

Fig. 3 Reaction energy profiles of CO oxidation on doped surface for pathway B (top) and pathway C (bottom).

For the doped system, formation of this intermediate is endothermic (+0.40 eV). Structurally, it corresponds to a CO molecule placed at 2.059 Å above the surface with the C-O bond slightly elongated (0.004 Å). Its fate is that of evolving to B6, which is a physisorbed CO_2 molecule identical to A5 (see Figure 2e).

The last examined pathway (C) shares the first two steps with the other ones (see Figure 3, bottom) and is adapted from a scheme previously proposed for doped ceria.[9] The mechanism is characterized by the adsorption of O_2 at the vacancy site in an almost symmetrical η^2 configuration. This reacts with a CO molecule forming an inverted [CO_3] intermediate,[7] which is in turn decomposed, forming molecularly adsorbed CO_2. As for pathway B, stable intermediates were found only for the doped system. Moreover, in comparison with the previous cases, the O_2 intermediate (C4, see Figure 2c) is less stable by 0.12 eV, which is a first evidence against the viability of the C pathway. In addition, the CO_2 subsequently formed (C5) is indeed a carbonate-like species, being strongly bent (133°), and having the internal C-O bonds stretched by almost 0.1 Å. Not unexpectedly, this species is strongly bound to the surface (ΔE_{ads} = 1.06 eV). As the formation of carbonate species is not observed experimentally,[15] this represents a further proof that pathway C is not suitable to describe the actual reaction of the catalytic reaction.

Different cobalt spin states (doublet, quartet, and sextet) are investigated for all the intermediates reported in Figures 1 and 3. When adsorbates are absent (e.g., A1 and A3) or interact weakly with the surface (A5), the most stable spin state is a quartet. However, the quartet and sextet states are very close in energy. In contrast to that, adsorption of a stronger ligand such as CO on the Co atom (A2 and B5) stabilizes a doublet state.

Summarizing, the main findings are that: i. the most endothermic step (A2 → A3) is by far the formation/desorption of the first CO_2 molecule, which forms an oxygen vacancy in the pure surface. *ii*. this step is instead exothermic for the Co-doped surface. *iii*. the A and B pathways have minor differences, the B pathway having an extra endothermic step (B4 → B5). *iv*. adsorption of O_2 in a η^2 configuration, involved in pathway C, is unfavoured wrt a terminal geometry. *v*. the C pathway includes a significantly endothermic step (C5 → C1) one, involving the desorption of stable carbonate-like CO_2 species, whose desorption is energetically unfavourable,[38] and its presence has not been detected experimentally. *vi*. in addition, barriers are expected to be negligible when adsorption/desorption of molecularly adsorbed species is involved (see e.g. a recent investigation on CO oxidation by Co_3O_4).[7]

On the basis of the above enumerated considerations we can safely limit our interest to pathway A, whose only likely rate determining step is, in the case of pure $SrTiO_3$, the O abstraction by adsorbed CO molecules, viz. the A2 → A3 step. Thus, we decided to locate and compare the transition states of this step for the pure and for the doped systems. The energy barriers (see Figure 4) are computed to be 1.65 eV and 0.15 eV, respectively, which confirms that the experimentally observed catalytic properties of the Co-doped material can be ascribed to the drastic increase of O vacancies formation/CO oxidation rate due to the insertion of Co at a high oxidation state on the surface. Looking to the process in closer detail, we remark that, on pure $SrTiO_3$, the CO adsorption on the Ti atom does not change the spin state of the surface. On the other hand, the CO oxidation induces a reduction of the surface, and releases two electrons to the conduction band. The most stable electronic configuration is obtained when the two Ti atoms close to the vacancy are reduced to Ti (III), and when a triplet state is formed. Because the A1→A2 step is very endothermic in the pure system, we expect that the transition state will be geometrically close to the product. We computed the potential energy surface for both singlet and triplet states. The TS is localized on the singlet PES and corresponds to the formation of a bond between the adsorbed CO molecule and a neighbouring surface O anion. As above pointed out, in the doped surface the A2 → A3 step is very exothermic, which suggests an early transition state. In this case, the adsorption of CO leaves the cobalt atom in a low spin state which is conserved after the transition state.

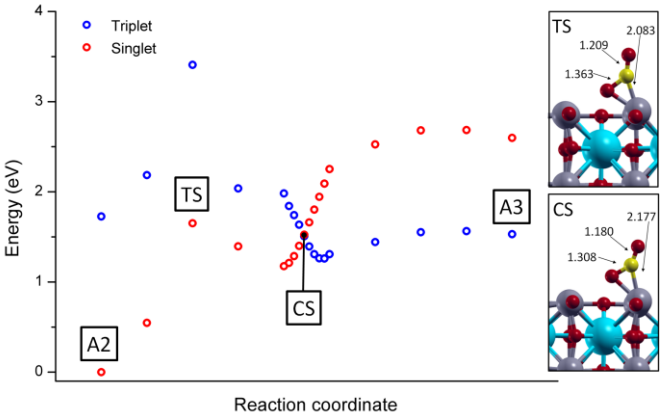

Fig. 4. Singlet and triplet PES for the vacancy formation step (A2 → A3) at the $SrTiO_3$ (100) surface.

4. Conclusions

In conclusion, we have adapted to Co-doped $SrTiO_3$, a complex oxide system, the catalytic cycles devised to describe CO oxidation on simple metal oxides. By examining the stability of the intermediate species, we find that one of the proposed mechanisms involves only exothermic steps (except for the desorption of loosely-bound molecular species), and is well-suited to describe the reaction mechanism. Furthermore, we have obtained evidence that the main effect through which Co doping enhances the catalytic properties of $SrTiO_3$ is the drastic lowering (1.5 eV) of the energy barrier for the abstraction of surface O atoms by adsorbed CO molecules. This is reflected in the enthalpy change for this step, which turns from strongly endothermic (+1.25 eV) to strongly exothermic (-1.19 eV), whereas all the other steps are scarcely affected by doping. Catalyst deactivation by the formation of carbonates is avoided because the formation of precursor η^2-O_2 species at the vacancy sites is unflavoured with respect to η^1-O_2, which brings instead to the desired product. Overall, our results show that the

vacancy formation energy is likely to be a good descriptor for the catalytic activity of doped perovskite systems in CO oxidation.

Acknowledgments

The research leading to these results has received funding from the European Union's 7th Framework Programme under grant agreement no 280890- NEXT-GEN-CAT and by MIUR of Italy through PRIN project DESCARTES (n. 2010BNZ3F2). Calculations are performed at the LICC ("Laboratorio Interdipartimentale di Chimica Computazionale") HPC facility of the Dipartimento di Scienze Chimiche of the Università degli Studi di Padova and at the CRI, HPC facilty of the Lille Universty (partially fonded by Feder)

References

1. S. Royer, D. Duprez, *ChemCatChem*, 2011, **3**, 24-65.
2. S. Azad, M.H. Engelhard, L.Q. Wang, *J. Phys. Chem. B*, 2005, **109**, 10327-10331.
3. Y.F. Yu Yao, *J. Catal*., 1984, **87**, 152-162.
4. H.Y. Kim, H.M. Lee, G. Henkelman, *J. Am. Chem. Soc.*, 2012, **134**, 1560-1570.
5. X.L. Xu, E. Yang, J.Q. Li, W.K. Chen, *ChemCatChem*, 2009, **1**, 384-392.
6. M. Nolan, *J. Chem. Phys.*, 2009, **130**, 144702 (1-9).
7. X.Y. Pang, C. Liu, D.C. Li, C.Q. Lv, G.C. Wang, *ChemPhysChem*, 2013, **14**, 204-212.
8. P. Broqvist, I. Panas, H. Persson, *J. Catal*., 2002, **210**, 198-206.
9. V. Shapovalov, H. Metiu, *J. Catal*., 2007, **245**, 205-214.
10. S. Chrétien, H. Metiu, *Catal. Lett*., 2006, **107**, 143-147.
11. M.A. Pena, J.L.G. Fierro, *Chem. Rev*., 2001, **101**, 1981-2017.
12. Y. Zhang-Steenwinkel, L.M. van der Zande, H.L. Castrum, A. Bliek, *Appl. Catal. B*, 2004, **54**, 93-103.
13. P.D. Petrolekas, I.S. Metcalfe, *J. Catal*., 1995, **152**, 147-163.
14. P.D. Petrolekas, I.S. Metcalfe, *J. Catal.*, 1995, **157**, 545-549.
15. A. Glisenti, M.M. Natile, S. Carlotto, A. Vittadini, *Catal. Lett.*, 2014, **144**, 1466-1471.
16. H.J. Zhang, G. Chen, Z.H. Li, *Appl. Surf. Sci.*, 2007, **253**, 8345-8351.
17. J.A. Rodriguez, S. Azad, L.Q. Wang, J. Garci, A. Etxeberria, L. Gonzalez, *J. Chem. Phys*., 2003, **118**, 6562-6569.
18. J.N. Yun, Z.Y. Zhang, J.F. Yan, F.C. Zhang, *Chin. Phys. Lett*., 2010, **27**, 017101 (1-4).
19. R.A. Evarestov, A.V. Bandura, V.E. Alexandrov, *Surf. Sci*., 2007, **601**, 1844-1856.
20. V. Alexandrov, S. Piskunov, Y.F. Zhukovskii, E.A. Kotomin, J. Maier, *Integr. Ferroelectr.*, 2011, **123**, 18-25.
21. H. Guhl, W. Miller, K. Reuter, *Phys. Rev. B*, 2010, **81**, 155455 (1-8).
22. S. Carlotto, M.M. Natile, A. Glisenti, A. Vittadini, *Surf. Sci.*, 2015, **633**, 68-76.
23. J.P. Perdew, K. Burke, M. Ernzerhof, *Phys. Rev. Lett*., 1996, **77**, 3865-3868.
24. Studies of adsorption of NO, CO, and O_2 molecules on the same systems investigated here show that differences between PBE and PBE+U calculations are small and certainly acceptable for our purposes.[22]
25. S. Carlotto, M.M. Natile, A. Glisenti, A. Vittadini, *Chem. Phys. Lett.*, 2013, **588**, 102-108.
26. P. Giannozzi *et al.*, *J. Phys. Condens. Matter*, 2009, **21**, 395502 (1-19).
27. https://www.vasp.at/
28. (a) P.E. Blöchl, *Phys. Rev. B*, 1994, **50**, 17953-17979; (b) G. Kresse, J. Joubert, *Phys. Rev. B*, 1999, **59**, 1758-1775.
29. (a) G. Henkelman and H. Jónsson, *J. Chem. Phys.*, 2000, **113**, 9901-9904; (b) G. Henkelman and H. Jónsson, *J. Chem. Phys.*, 2000, **113**, 9978-9985.
30. J.M.D. Tascon, J.L.G. Fierro, L.G. Tejuca, *Zeit. Phys. Chem. NeueFolge*, 1981, **124**, 249-257.
31. R.J. Voorhoeve, D.W. Johnson, J.P. Remeika, P. K. Gallagher, *Science*, 1977, **195**, 827-833.
32. K.A. Chan, J. Ma, S. Jaenicke, G.K. Chuah, J. Lee, *Appl. Catal. A*, 1994, **107**, 201-227.
33. E.W. McFarland, H. Metiu, *Chem. Rev.*, 2013, **113**, 4391-4427.
34. P. Mars, D.W. van Krevelen, *Chem. Eng. Sci. Spec. Suppl.*, 1954, **3**, 41-57.
35. Z. Yang, Z. Lu, G. Luo, K. Hermansson, *Phys. Lett. A*, 2007, **369**, 132-139.
36. G. Dutta, U.V. Waghmare, T. Vaidya, M.S. Hedge, K.R. Priolkar, P.R. Sarode, *Catal. Lett.*, 2006, **108**, 165-172.
37. M. Nolan, V. Soto, H. Metiu, *Surf. Sci.*, 2008, **602**, 2734-2742.
38. S. Carlotto, M.M. Natile, A. Glisenti, A. Vittadini, *Appl. Surf. Sci.*, 2016, **364**, 522-527.